# Analytical treatment of the interaction between light, plasmonic and quantum resonances: quasi-normal mode expansion

Mathias Perrin, J. Yang, P. Lalanne

# Analytical treatment of an interaction between light, plasmonic and quantum resonances:

# The quasi-normal mode expansion

M. Perrin[a], J. Yang[b], P. Lalanne [b]
[a] Univ. Bordeaux, LOMA, UMR 5798, F-33400 Talence, France
[b] Univ. Bordeaux, LP2N, F-33400 Talence, France

## ABSTRACT

We summarize here, and detail with numerical examples, the Quasi-Normal Mode theory which has been developed in a recent series of papers dealing with classical and quantum plasmonics. We present the semi-analytical formalism capable of handling the coupling of electromagnetic sources, such as point dipoles or free-propagating fields, with various kinds of dissipative and dispersive resonators. Due to its analyticity, the approach is very intuitive, and very versatile and can be applied to canonical problems of quantum optics and sensing with nanoresonators.

**Keywords:** Quasi-Normal Modes, Quantum Plasmonics, Sensing

## 1. INTRODUCTION

Plasmonic resonators made of metallic nanoparticles (NP) are very appealing devices as they permit to concentrate light fields at the nanometer scale. In this regime, where quantum and classical world meet[1,2] , both fundamental and applied research have been recently developed. Let us mention, in particular, new light sources (nano-lasers) or light routing devices (nano-switches). A priori, one would naturally lean on brute force numerical simulation to compute the key physical quantities ( e.g. cross sections, Purcell factors), and make designs. However, this is hard to do in practice. One would indeed need to repeat many independent computations, when parameters such as wavelength, polarization, … are changed. Besides, much knowledge about the physical mechanisms at play remains hidden.

To go beyond such limitation, we have developed a modal method[3,4] that permits to obtain easily an accurate prediction, of the fields in or around the resonator. To do this, we expand the fields on the quasi-normal modes of the resonator, whose eigenfrequency is a complex number. Once the modes have been computed numerically, and properly normalized, their excitation coefficient is known analytically, even for three-dimensional, open and dispersive problems. In addition to providing a simple solution of canonical systems (nanoparticle on substrate, plasmonic nano-antenna, …), the modal approach permits a smart and physical analysis of complex situations, especially when several modes are at play. In a first section, we present the formalism and discuss it on an example where three resonances are involved. In second section, we recall how QNM expansion can be useful to treat hybrid atom/NP systems[5] . Going back to classical physics, we then discuss a topical application : the design of devices for plasmonic sensing[6].

## 2. OVERLOOK OF QNM THEORY

The rationale behind QNM theory is the expansion of electromagnetic fields onto the modes of the nanoresonators, *and* the analytic computation of their excitation coefficients. While electromagnetic modes of macroscopic resonators – e.g. Fabry-Perot and ring cavity – are known analytically, and have simple expression[7], this is not the case for NP electromagnetic modes. One need to compute them numerically in the general case of a nanoresonator, made of possibly dispersive and dissipative material. Mathematically speaking, one searches for the solutions of the Maxwell equations without source,

$$\nabla \times \tilde{\mathbf{E}}_m = -\mathrm{i}\, \tilde{\omega}_m\, \boldsymbol{\mu}(\mathbf{r},\tilde{\omega}_m)\, \tilde{\mathbf{H}}_m\,, \tag{1a}$$

$$\nabla \times \tilde{\mathbf{H}}_m = \mathrm{i}\, \tilde{\omega}_m\, \boldsymbol{\varepsilon}(\mathbf{r},\tilde{\omega}_m)\, \tilde{\mathbf{E}}_m\,. \tag{1b}$$

There, $\tilde{\omega}_m ; \tilde{\mathbf{E}}_m ; \tilde{\mathbf{H}}_m$ are respectively the eigenfrequency of the m[th] QNM, its Electric and Magnetic eigenfield. For a metallo-dielectric nanoresonator, this generalized eigenvalue problem admits complex numbers for the $\tilde{\omega}_m$. This is due to the fact the problem is dissipative – the metal absorbs, and the system is open: energy leaks to infinity. The imaginary part of $\tilde{\omega}_m$ is indeed linked to the losses per unit of time in the system. More precisely, the quality factor of the m[th] mode is approximately given by $Q = \mathrm{Re}(\tilde{\omega})/[2\,\mathrm{Im}(\tilde{\omega})]$. Notice that this relationship is very interesting, as the sole knowledge of $\tilde{\omega}_m$ already permits to approximate Q, without making any (lengthy) computation of cross section or Purcell factor.

If one wants to go further, however, and obtain quantitative expressions, one will seek to expand the field on the modes. Then, one has to face a mathematical difficulty: eqs.(1) cannot be described by an Hermitian operator, and no formalism as simple as the theory of auto-adjoint operators can be used to treat the problem. An assumption of total field expansion has however proven to be helpful in many cases. Either the total field[3] or the scattered[4] field can be expanded as a sum of modes – note that both fields are similar close to the NP resonances. One writes

$$\boldsymbol{\Psi}(\mathbf{r},\omega) \approx \sum_m \beta_m(\omega)\, \tilde{\boldsymbol{\Psi}}_m(\mathbf{r}), \tag{2}$$

Where $\boldsymbol{\Psi}(\mathbf{r},\omega) \equiv [\mathbf{E}(\mathbf{r},\omega), \mathbf{H}(\mathbf{r},\omega)]$ is either the ( scattered or total ) field one wants to expand. In practice, to use Eq. (2), one absolutely needs to define normalized modes, that do not depend on the excitation conditions. This is one of the main difficulty. Indeed, it turns out that both fields $\tilde{\mathbf{E}}_m(\mathrm{r}); \tilde{\mathbf{H}}_m(\mathrm{r})$ are always diverging exponentially, going away from the scatterer[3,4] . Then, even if one can compute the field profile inside, or around the NP, it is impossible to normalize the modes in the usual sense (for example by imposing a unitary value for their total energy integrated on the whole space). This problem was solved by using an analytical continuation of the diverging field[3], which permitted to define rigorously the *normalized* Quasi-Normal modes (hereafter referred as the QNM or quasi-normal modes), and by proposing a numerical method based on the use of PMLs to help computing analytical quantities such as the mode volume.

To find the normalized modes, Eqs. (1.a,b) can be solved with commercial Finite Element solvers. However, with metallic nanoparticles, whose permittivity is frequency dependent, the eigenvalue problem becomes non-linear, and a specific iterative method turns out to be more efficient[4]. Note that this latter improvement do not necessitate to integrate the field inside the PMLs. Eventually, each mode is normalized independently, and the total (or scattered) field is expressed as a sum of modes. The expression for the excitation coefficient of the scattered field, $\beta_m(\omega)$ , is obtained as[4]:

$$\beta_m(\omega) = \frac{-\omega \iiint \Delta\boldsymbol{\varepsilon}(\mathbf{r},\omega)\mathbf{E}_b(\mathbf{r},\omega)\cdot \tilde{\mathbf{E}}_m(\mathbf{r})\,d^3\mathbf{r}}{(\omega - \tilde{\omega}_m)}, \tag{3}$$

And then the total field is finally

$$\boldsymbol{\Psi}(\mathbf{r},\omega) \approx \boldsymbol{\Psi}_b(\mathbf{r},\omega) + \sum_{m=1}^{3} \beta_m(\omega)\tilde{\boldsymbol{\Psi}}_m(\mathbf{r}), \tag{4}$$

where $\boldsymbol{\Psi}_b(\mathbf{r},\omega)$ is the background field $\boldsymbol{\Psi}_b(\mathbf{r},\omega) \equiv [\mathbf{E}_b(\mathbf{r},\omega), \mathbf{H}_b(\mathbf{r},\omega)]$, imposed by the external condition (light beam, field excited by a point source, …). $\Delta\boldsymbol{\varepsilon}(\mathbf{r},\omega)$ is the difference between the metal and surrounding environment permittivity. In our simulations, we use a Drude model, $\varepsilon_{Au} = 1 - \omega_p^2/(\omega^2 - i\omega\gamma)$, with $\omega_p = 1.26\times10^{16}\,s^{-1}$ and $\gamma = 1.41\times10^{14}\,s^{-1}$, to define an analytical continuation of the gold permittivity for complex frequencies. The values of $\omega_p$ and $\gamma$ are fitted from tabulated data in[8], and $\boldsymbol{\mu}(\mathbf{r},\omega)$ is simply equal to the permeability of the vacuum. In this section, we will study a cylindrical nano-resonator made of gold, of length L=200 nm and diameter D=30 nm. Table 1 gathers the three main QNMs for wavelength between 0.5 µm and 2.5 µm.

| | | |
|---|---|---|
| Mode 1 | $\lambda_1$=1.5-0.098i µm | Symmetric along Z axis |
| Mode 2 | $\lambda_2$=0.8-0.023i µm | Anti-symmetric along Z axis |
| Mode 3 | $\lambda_3$=0.6-0.013i µm | Symmetric along Z axis |

Table 1 : properties of the QNM modes used to model the cylindrical gold nanorod of length L=200 nm and diameter D=30 nm.

### 2.1 Purcell factor

Once the QNM are known, physically meaningful quantities, such as the Purcell factor of a dipole placed close to the nanoresonator can be evaluated easily. Figure 1 shows the spectral evolution of such Purcell factor. It is spectacular to observe that we need only three QNMs to obtain a very good quantitative agreement on such a large spectral window, both on and aside the resonances. One can notice that the strongest peak is due to the coupling of the point dipole (oriented along Z axis), with the field $\iiint \tilde{\mathbf{E}}_1(\mathbf{r})\,d^3\mathbf{r}$, which is also mainly oriented in this direction (mode 1 is the Z-dipolar mode of the nanoparticle). For the second peak (around λ=0.8 µm), $\iiint \tilde{\mathbf{E}}_2(\mathbf{r}) \bullet \mathbf{u}_\mathbf{Z}\,d^3\mathbf{r} = 0$ as the second QNM is antisymmetric (see the inset in Figure 1). There, coupling occurs with the X and Y components of the QNM, and gives a much less intense peak.

### 2.2 Scattering, Absorption, Extinction cross sections

Another set of important physical quantities is the absorption, extinction, and scattering cross section. Let us show here how one can obtain the absorption cross section from quasi-normal mode expansion Eq.(2). We have used the relation:

$$\sigma_A = -\frac{1}{2S_0}\iiint_V \mathrm{Im}(\omega\varepsilon(\mathbf{r},\omega))\left|\mathbf{E}_S(\mathbf{r},\omega) + \mathbf{E}_b(\mathbf{r},\omega)\right|^2 \mathbf{d}^3\mathbf{r}\,, \tag{5}$$

that permits to express the absorption cross section as a function of a volume integral on the NP [4]. Figure 2 shows the spectral evolution, dominated by only two out of the three quasi-normal modes. This feature is due to the fact that mode number 2 is antisymmetric, *and* the excitation is now made by a plane wave, so that $\beta_2(\omega) \prec \iiint \tilde{\mathbf{E}}_2(\mathbf{r}) \bullet \mathbf{u}_\mathbf{Z}\,d^3\mathbf{r} \approx 0$. Then, this mode do not contribute to the absorbed field (when it is excited by such plane wave). This is why Purcell

factor and Absorption cross section do not show the same number of resonances. Of course, things would be different if the incidence angle of the plane wave changes.

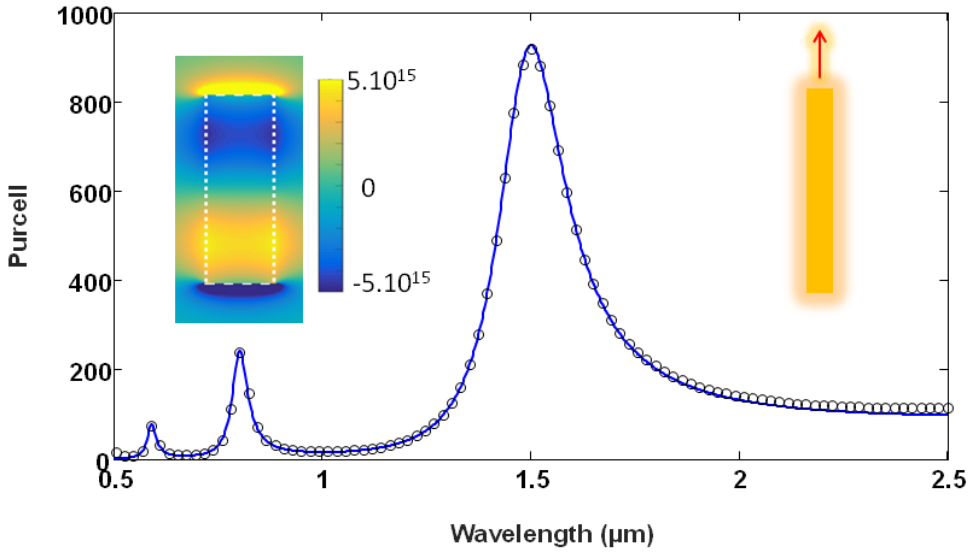


Figure 1 : Purcell factor of a dipole placed in the vicinity of a gold cylinder of 200nm length and 30 nm diameter. The dipole is located at 10 nm of the cylinder, on its axis, and oriented along the axis (see the inset). Three modes have been considered and assumed to be orthogonal (blue line), the symbols display the exact FEM calculation. In particular, an antisymmetric mode is excited. Its normalized QNM profile – real part of Ez field, along the rod axis – is shown in the inset.

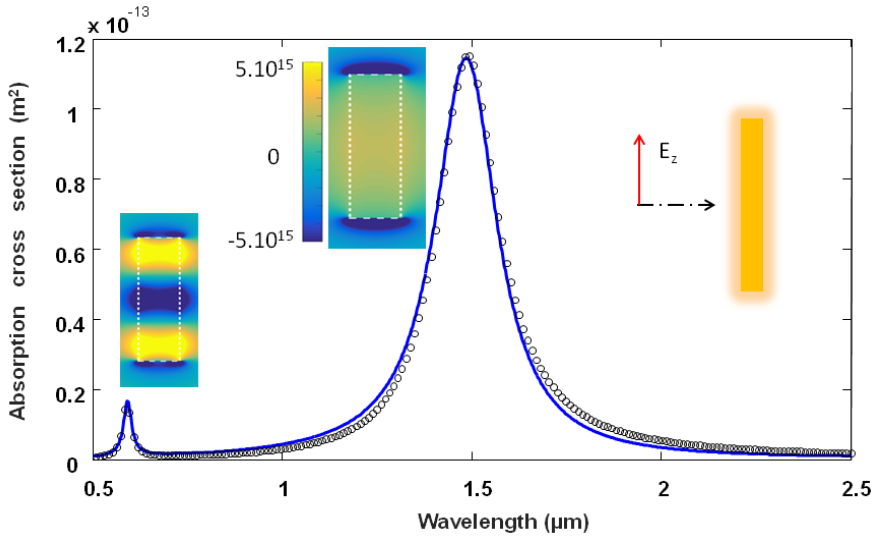


Figure 2 : Absorption cross section of a gold cylinder of 200nm length and 30 nm diameter excited by a plane wave polarized along the rod axis, and propagating perpendicular to it (see inset). Three modes have been considered and assumed to be orthogonal (blue line), the symbols display the exact FEM calculation. Apart from the antisymmetric mode of Figure 1 (not excited here), two other symmetric modes have been represented. The insets show the real part of Ez.

## 3. QNM THEORY APPLIED TO QUANTUM PLASMONICS

We have seen in the previous section that two key physical quantities, the Purcell factor and the cross sections, can be modeled quite precisely by a QNM expansion. At first sight, these quantities belong to classical physics, but they can be very useful for describing nanostructured quantum systems. Indeed, the seminal quantum works[9] has been derived in free space. In order to transpose those theories to quantum resonators lying in the vicinity of nanoparticles, it is essential to know how the density of state is modified by the presence of a NP, and how the far field emission is affected by absorption or scattering of the NP.

Using a simple semi-classical theory, we can describe[9,10] an hybrid system made of an atom or quantum dot (modeled by an induced dipole) and coupled to a NP. Upon some hypotheses (weak coupling, small enough driving intensity), the spectral response of the system is linear, and can be described in very simple and generic terms[5].

### 3.1 QNM formalism for quantum nano-optics

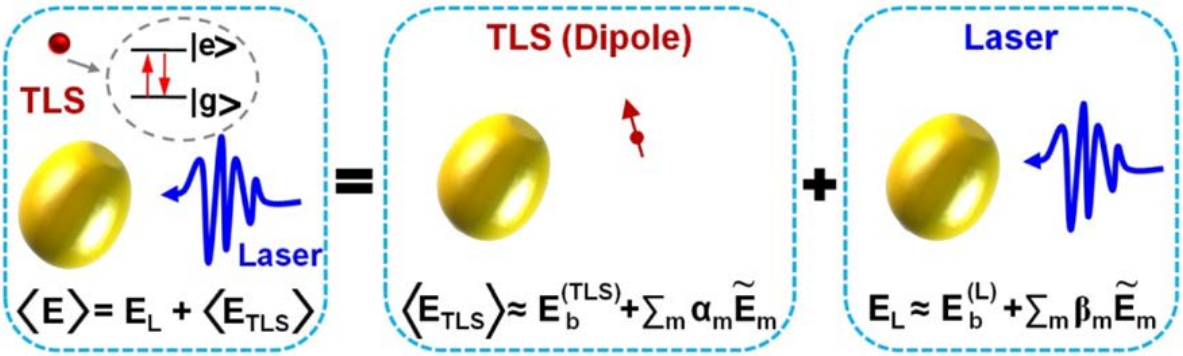


Figure 3 : Overview of the semi-analytical modal formalism. The response of the hybrid system (left) to the laser driving field results from two contributions, the field radiated by the two level system (TLS) with modal expansion coefficients denoted $\alpha_m$ and the field due to the driving excitation with modal expansion coefficients denoted $\beta_m$.

$\mathbf{E}_b^{(TLS)}(\mathbf{r})$ and $\mathbf{E}_b^{(L)}(\mathbf{r})$ are respectively the background field associated to the TLS response and the external driving field excitation, in the absence of the nanoresonator.

The atom is modeled by an electric dipole moment, which reads, neglecting Rabi broadening,

$$< \mathbf{d} >= \frac{-\boldsymbol{\mu}_{eg}\tilde{\Omega}^*}{2\tilde{\delta}_L - \mathrm{i}}, \tag{6}$$

There, $\gamma$ describes the rate of spontaneous emission is directly related to the Purcell factor. $\tilde{\delta}_L$ is the detuning between atom resonance frequency and injected field frequency, normalized to the Purcell broadened linewidth $\gamma$. The Rabi frequency (normalized by $\gamma$), $\tilde{\Omega}$, is proportional to the injected field in the presence of NP and absence of atom. At the difference with Section 2., the dipole has now its own lineshape, and is not a monochromatic emitter. Eventually, we demonstrated that the interplay of a fine atomic and the broad plasmonic resonance creates a Fano spectral profile, whose shape can be well approximated by the analytical expression ,

$$F_m\left(\tilde{\delta}_L\right) = \frac{2\tilde{\delta}_L + i(f_m - 1)}{2\tilde{\delta}_L - i}, \tag{7}$$

where $f_m$ is a modal Fano coefficient, that is computed simply and directly from the QNM properties[5]. Depending on $f_m$, one can obtain many types of Fano lineshapes $F_m\left(\tilde{\delta}_L\right)$ going from a Lorentzian to more complex responses, and link them to some physical situation (small / strong Purcell, e.g.) [5]. The quantity $F_m\left(\tilde{\delta}_L\right)$ is proportional to the scattering or extinction cross section, and permits to have rapidly a clear idea of how the device would behave when such and such parameters are varied (typically the detuning between atom resonance and injected frequency, the atom location). Figure 4, panel (a) shows such profile (both exact and QNM expansion), where a hole is burn in the broad local plasmonic resonance. The advantage of QNM to handle this problem is that the result can be applied virtually to any shape of the NP, and is general, even if the resonator supports several QNMs [5].

### 3.2 Fano response of an hybrid system and associated radiation diagram

Since the field scattered by the system is expanded as a sum of QNMs, one can also compute all the far field properties of the hybrid system very rapidly, for any detuning $\tilde{\delta}_L$. Figures 4 (b) and (c) show the far field radiation diagram for different detunings ($\tilde{\delta}_L$). It appears that the nanoresonator permits to control the direction and polarization of emitted plane wave with the wavelength of injected plane wave.

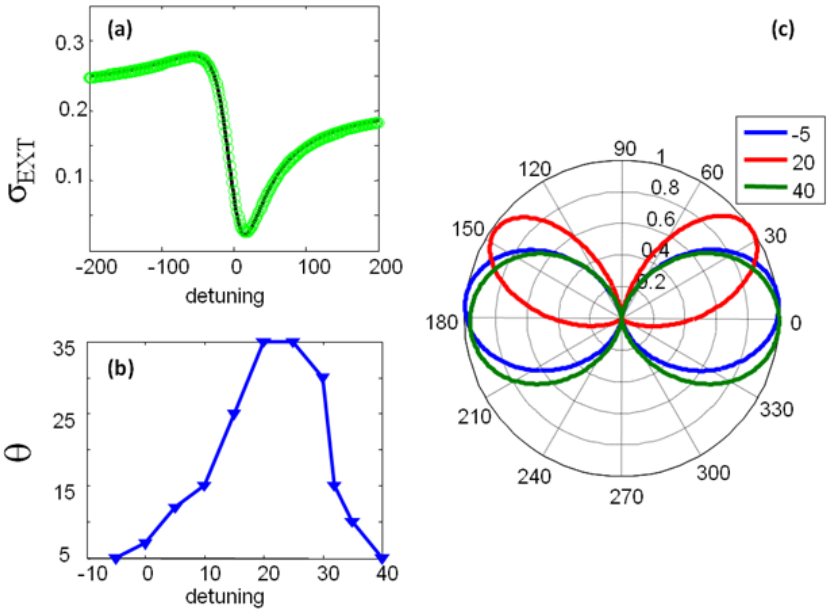


Figure 4 : Optical properties of an hybrid system made of a silver nanosphere of 20nm radius coupled to a quantum dot, modeled as an induced dipole, whose lineshape is given by Eq.(4). The dipole is oriented radially, placed at 20 nm above the sphere, and the hybrid system is excited by a plane wave propagating in a direction perpendicular to the dipole, and polarized along the dipole direction. Panel **(a)** shows the extinction cross section of the hybrid system, as a function of the detuning between quantum dot resonance and plane wave frequency. Detuning is normalized to the Purcell broadened linewidth $\gamma$. Panel **(c)** shows the far field radiation diagram of the structure, in a plane perpendicular to the dipole axis, for 3 values of the detuning. Panel **(b)** shows how the direction of maximal emission varies with the normalized detuning.

In a similar way, the formalism can be extended to handle hybrid systems composed of a discrete ensemble of TLSs and a single resonator, and to study the reinforcement of cooperative electromagnetic effects between the oscillators due to the interaction with the nanoresonator[11] . We have recently shown that the implementation of the QNM formalism is of crucial importance for the description of the electromagnetic response of such hybrid systems with arbitrarily shaped nanoresonators and that the semi-analyticity of the approach leads to a substantial reduction of the computational time.

## 4. QNM THEORY APPLIED TO BIO-SENSING

### 4.1 Perturbation of a resonance

Because metallic nanoparticles support spatially highly confined resonances that is usually accompanied with strong near field, they can effectively convert the changes of refractive index (more generally, permittivity and/or permeability) in their vicinity into frequency shifts of the resonance. Significant development in sensing technologies has been achieved in the recent years based on localized surface plasmon resonance of metallic nanoparticles[12]. Note that both the frequency shift $\mathrm{Re}(\Delta\tilde{\omega})$ and the resonance broadening $-2\mathrm{Im}(\Delta\tilde{\omega})$ are two fundamental quantities relevant for sensing applications. However, usually these two quantities can only be predicted by repeated fully-vectorial electromagnetic calculations. A simple and analytical (or semi-analytical) formula accurate for photonic or plasmonic nanoresonators of arbitrary size and shape, potentially composed of lossy and dispersive materials, is essentially important, but has not been already established.

In this section, based on rigorous treatment of quasi-normal mode (QNM) normalization introduced in Section 2, we derive a close-form expression that can accurately predict the complex-valued shift $\Delta\tilde{\omega}$ of the eigenfrequency $\tilde{\omega}$ of a resonance due to the presence of a perturbation, which is a local variation of refractive index (or permittivity or permeability) in the vicinity of the resonator (see Fig. 5a). Then the accuracy of the semi-analytical formula is shown with a canonical example in plasmonic sensing. More details and examples can be found in a recent publication[6]. Considering two slightly different system as shown in Fig. 5a,

### 4.2 Derivation of the master equation

Here we outline the major steps to derive a closed-form expression of $\Delta\tilde{\omega}$, for the case with a permittivity perturbation. The formula can be extended to general cases with both permittivity and permeability perturbations. Two eigenvalue problems are associated to the refractive-index sensing configuration (see Fig. 5a): the first corresponds to an eigenmode of the bare metallic nanoresonator and the second corresponds to the eigenmodes of the same nanoresonator dressed by a perturbation. Let us denote the eigensolutions to the Maxwell's equations for these two problems as $\left(\nabla\times\tilde{\mathbf{E}}=-i\tilde{\omega}\boldsymbol{\mu}\tilde{\mathbf{H}},\nabla\times\tilde{\mathbf{H}}=i\tilde{\omega}\boldsymbol{\varepsilon}\tilde{\mathbf{E}}\right)$ and $\left(\nabla\times\tilde{\mathbf{E}}'=-i\tilde{\omega}'\boldsymbol{\mu}'\tilde{\mathbf{H}}',\nabla\times\tilde{\mathbf{H}}'=i\tilde{\omega}'\boldsymbol{\varepsilon}'\tilde{\mathbf{E}}'\right)$, respectively. The two solutions have slightly different eigenfrequencies, $\tilde{\omega}$ and $\tilde{\omega}'$. Applying the divergence theorem to the vector $\tilde{\mathbf{E}}'\times\tilde{\mathbf{H}}-\tilde{\mathbf{E}}\times\tilde{\mathbf{H}}'$, we obtain

$$\iint_{\Sigma}\left(\tilde{\mathbf{E}}'\times\tilde{\mathbf{H}}-\tilde{\mathbf{E}}\times\tilde{\mathbf{H}}'\right)\bullet d\mathbf{S}=-i\iiint_{\Omega}\left\{\tilde{\mathbf{E}}\bullet\left[\tilde{\omega}\boldsymbol{\varepsilon}(\tilde{\omega})-\tilde{\omega}'(\boldsymbol{\varepsilon}(\tilde{\omega}')+\Delta\boldsymbol{\varepsilon}(\tilde{\omega}'))\right]\tilde{\mathbf{E}}'-\tilde{\mathbf{H}}\bullet\left[\tilde{\omega}\boldsymbol{\mu}(\tilde{\omega})-\tilde{\omega}'\boldsymbol{\mu}'(\tilde{\omega}')\right]\tilde{\mathbf{H}}'\right\}d^3\mathbf{r}\,, \tag{8}$$

where $\Delta\boldsymbol{\varepsilon}(\tilde{\omega}')$ denotes the permittivity change induced by the perturbation, i.e., $\Delta\boldsymbol{\varepsilon}(\omega)=\boldsymbol{\varepsilon}_{\mathrm{p}}(\omega)-\boldsymbol{\varepsilon}_{\mathrm{b}}(\omega)$ with $\boldsymbol{\varepsilon}_{\mathrm{p}}$ and $\boldsymbol{\varepsilon}_{\mathrm{b}}$ denoting the permittivities of perturbation and background medium. In Eq. (1), $\sum$ is a closed surface defining a volume $\Omega$. The volume integral in Eq. (1) can be evaluated over the whole space $\Omega$, consisting of two sub-domains $\Omega_1$ and $\Omega_2$. $\Omega_1$ denotes a finite-volume real space that contains the metallic nanoparticle, and $\Omega_2$ denotes PMLs (relevant detailed discussions can be found in Section 2 and Ref. [3]). Because of the exponential damping of field inside PMLs, the left-side of Eq. (2) becomes null, and assuming that $\Delta\tilde{\omega}=\tilde{\omega}'-\tilde{\omega}$ is small enough that we may adopt a 1st order expansion of the permittivity and permeability for $\omega\approx\tilde{\omega}$, Eq. (1) becomes,

$$\Delta\tilde{\omega} = \tilde{\omega}' - \tilde{\omega} = -\frac{\tilde{\omega}\iiint_{V_p} \Delta\boldsymbol{\varepsilon}(\mathbf{r},\tilde{\omega})\tilde{\mathbf{E}}'(\mathbf{r})\cdot\tilde{\mathbf{E}}(\mathbf{r})d^3\mathbf{r}}{\iiint_{\Omega}\left\{\tilde{\mathbf{E}}(\mathbf{r})\cdot\frac{\partial[\omega\boldsymbol{\varepsilon}(\mathbf{r},\omega)]}{\partial\omega}\tilde{\mathbf{E}}'(\mathbf{r}) - \tilde{\mathbf{H}}(\mathbf{r})\cdot\frac{\partial[\omega\boldsymbol{\mu}(\mathbf{r},\omega)]}{\partial\omega}\tilde{\mathbf{H}}'(\mathbf{r})\right\}d^3\mathbf{r}}, \quad (9)$$

Furthermore, we assume that the perturbation modifies the QNM field solely locally in a volume approximately equal to $V_p$, and that the error induced by replacing $\tilde{\mathbf{E}}',\tilde{\mathbf{H}}'$ by $\tilde{\mathbf{E}},\tilde{\mathbf{H}}$ into the denominator of Eq. (2) is negligible (the accuracy of this approximation has been tested in Ref. [6] with various examples). Then substituting the normalization introduced in in Ref. [3], $\iiint_{\Omega}\left\{\tilde{\mathbf{E}}\cdot\frac{\partial[\omega\boldsymbol{\varepsilon}]}{\partial\omega}\tilde{\mathbf{E}} - \tilde{\mathbf{H}}\cdot\frac{\partial[\omega\boldsymbol{\mu}]}{\partial\omega}\tilde{\mathbf{H}}\right\}d^3\mathbf{r} = 1$, into Eq. (3) we obtain

$$\Delta\tilde{\omega} = -\tilde{\omega}\iiint_{V_p}\Delta\boldsymbol{\varepsilon}(\mathbf{r},\tilde{\omega})\tilde{\mathbf{E}}'(\mathbf{r})\cdot\tilde{\mathbf{E}}(\mathbf{r})d^3\mathbf{r}. \quad (10)$$

To calculate the frequency shift $\Delta\tilde{\omega}$ using the sole knowledge of the unperturbed mode $\tilde{\mathbf{E}}$, we may adopt a practical approximation, $\tilde{\mathbf{E}}'(\mathbf{r}) \approx \alpha\varepsilon_b\tilde{\mathbf{E}}(\mathbf{r})/\left[V_p\Delta\boldsymbol{\varepsilon}(\mathbf{r},\tilde{\omega})\right]$, with $\alpha$ denoting the polarizability of the perturbing nano-object.

### 4.3 Numerical tests and discussion

For the sake of brevity, here we only show one test of the accuracy of the semi-analytical formula Eq. (3) for a canonical example: a cylindrical gold nanorod (radius $R$ = 10 nm and length $L$ = 80 nm) perturbed by individual nanospheres of varying sphere radius, as shown in Fig. 1(b). The excellent agreement between the model prediction and fully-vectorial calculations evidences the accuracy of the close-form expression, and more examples can be found in Ref. [6].

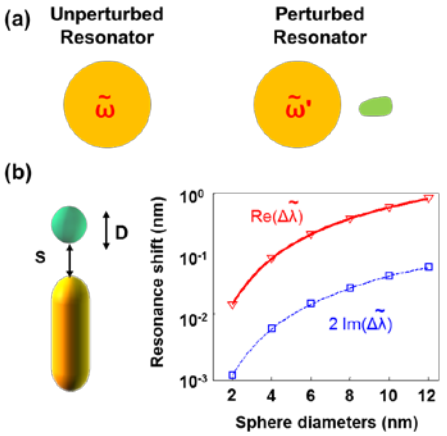


Figure 5. Resonance shifts of a gold nanorod due to the attachment of protein nanospheres ($n$ = 1.5) in aqueous environment ($n$ = 1.33). (**a**) Illustration of a bare metallic resonator (left) and a perturbed metallic resonator (right) due to the presence of a perturbing object (green). (**b**) *Re*( $\Delta\tilde{\lambda}$ ) and 2·*Im*( $\Delta\tilde{\lambda}$ ) as a function of the nanosphere diameter D for a fixed sphere-rod distance $S$ = 0.5nm. Triangle or square marks are obtained with fully-vectorial calculation and curves are predicted with Eq. (3).

We notice that there had been much effort to derive simple formulas, similar to Eq. (3), based on perturbation theory to predict frequency shifts of lossy and leaky resonators (including plasmonic resonators) due to perturbations[13-15]. The main difference resides in both the integrand used inside the formula, a $\tilde{\mathbf{E}}\cdot\tilde{\mathbf{E}}$ product instead of a $\tilde{\mathbf{E}}\cdot\tilde{\mathbf{E}}^*$ product and, of course, in the mode normalization. Replacing $\tilde{\mathbf{E}}\cdot\tilde{\mathbf{E}}^*$ by $\tilde{\mathbf{E}}\cdot\tilde{\mathbf{E}}$ is not just a small modification but has significant implications. Briefly, the use of $\tilde{\mathbf{E}}\cdot\tilde{\mathbf{E}}$ product and the mode normalization adopted here is mathematically rigorous for lossy and leaky resonances, and $\tilde{\mathbf{E}}\cdot\tilde{\mathbf{E}}$ product preserves the phase of the complex modal field, which is critical for predicting the spectral broadening $\mathrm{Im}(\Delta\tilde{\omega})$ due to perturbation. Additionally, based on large amount of simulations, we

find our proposed approach has much higher precision than the ones based on $\tilde{\mathbf{E}} \cdot \tilde{\mathbf{E}}^*$ products. Related discussion can be found in Ref. [6].

Finally, we would like to emphasize that the proposed approach is not restricted by the size or shape of the nanoresonators or perturbations. Also, it would be fascinating to extend the present work to multimode nanoresonators, such as complex systems supporting Fano-like resonances, which has been extensively studied for the bio-sensing applications.

## 5. CONCLUSION

We have presented, using a simple example, the QNM formalism recently developed, that is able to handle analytically the coupling between optical resonances and various kinds of sources, such as Dirac electrical dipoles or free-propagating fields. This formalism encompasses radiation leakage and Ohmic losses, and permits an accurate and fast description of major physical parameters such as Purcell factor and Cross sections. Application to hybrid systems made of quantum and classical resonator has been shown, which paves the way for a rigourous and simple treatment of nanolasers and other quantum nanodevices. Perturbative theory of QNM has also been developed with application to sensing. We believe the versatility of such description will make it a precious tool in nano-optics modeling.

## REFERENCES


[1] Schlather, A. E., Large, N., Urban, A. S., Halas, N. J. Nordlander, P., "Near Field mediated plexcitonic coupling and giant rabi splitting in individual metallic dimers", Nanolett. 13, 3281-3286 (2013).

[2] Tame, M. S., McEnery, K. R., Özdemir, S. K., Lee, J., Maier, S. A., Kim, M. S., "Quantum Plasmonics" , Nature Physics Vol **9**, 329 – 340 (2013).

[3] Sauvan, C., Hugonin, J. P., Maksymov, I. S., Lalanne, P., "Theory of the spontaneous optical emission of nanosize photonic and plasmon resonators", Phys. Rev. Lett. 110, 237401 (2013).

[4] Bai, Q., Perrin, M., Sauvan, C., Hugonin, J.P., Lalanne, P., "Efficient and intuitive method for the analysis of light scattering by a resonant nanostructure", Opt. Exp. 21 27371-27382 (2013).

[5] Yang, J., Perrin, M., Lalanne, P., "Analytical formalism for the interaction of two-level quantum systems with metal nanoresonators", Phys. Rev. X 5, 021008 (2015).

[6] Yang, J. Giessen, H., Lalanne, P. , "Simple analytical expression for the peak-frequency shifts of plasmonic resonances for sensing", Nano. Lett. , 15, 3439–3444 (2015).

[7] Siegman, A. E. , [Lasers], University Science Books, U.S. (1990). See in particular section 21.7.

[8] Palik, E. D., [Handbook of optical constants of solids], Academic Press, NY, Part II, (1985).

[9] Mandel, L., Wolf, E., [Optical coherence and quantum optics], Cambridge University Press (1995).

[10] Chen, X.-W. , Sandoghdar, V., Agio, M., "Coherent interaction of light with a metallic structure coupled to a single quantum emitter: from superabsorption to cloaking", Phys. Rev. Lett. 110, 153605 (2013).

[11] Pustovit, V. N., Shahbazyan, T.V., " Cooperative Emission of Light by an Ensemble of Dipoles Near a Metal Nanoparticle: The Plasmonic Dicke Effect", Phys. Rev. Lett. **102**, 077401 (2009).

[12] Anker, J.; Paige Hall, W.; Lyandres, O.; Shah, N.; Zhao, J.; Van Duyne, R. P. Nat. Mater., 7, 442−453 (2008).

[13] Waldron, R. A. Proc. Inst. Electr. Eng. 107C, 272 (1960).

[14] Arnold, S.; Khoshsima, M.; Teraoka, I.; Holler, S.; Vollmer, F. Opt. Lett. 28, 272 (2003).

[15] Koenderink, A. F.; Kafesaki, M.; Buchler, B. C.; Sandoghdar, V. Phys. Rev. Lett. 95, 153904 (2005).